Supporting Information:

Three-dimensional Si anodes with fast diffusion, high capacity, high rate capability, and long cycle life

Shailendra Chiluwal[1,2], Nawraj Sapkota[1], Apparao M Rao[1], and Ramakrishna Podila[1,2,*]

1. Clemson Nanomaterials Institute, Department of Physics and Astronomy, Anderson SC 29625 USA
2. Laboratory of Nano-biophysics, Clemson University, Clemson University, Clemson, SC 29634 USA

***Corresponding author: rpodila@g.clemson.edu**

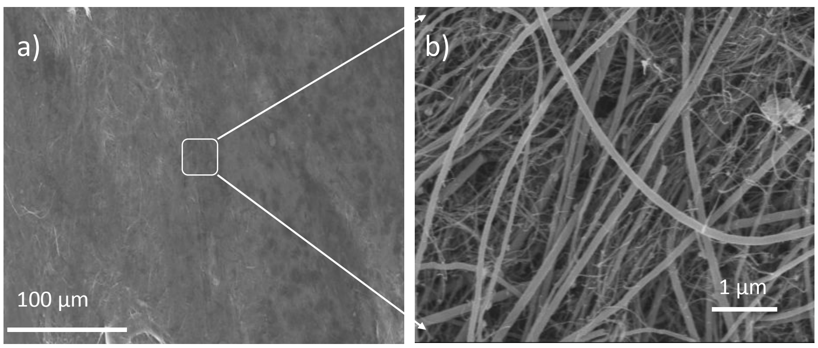

Figure S1: Electron micrographs of BPs used in this study at different magnifications.

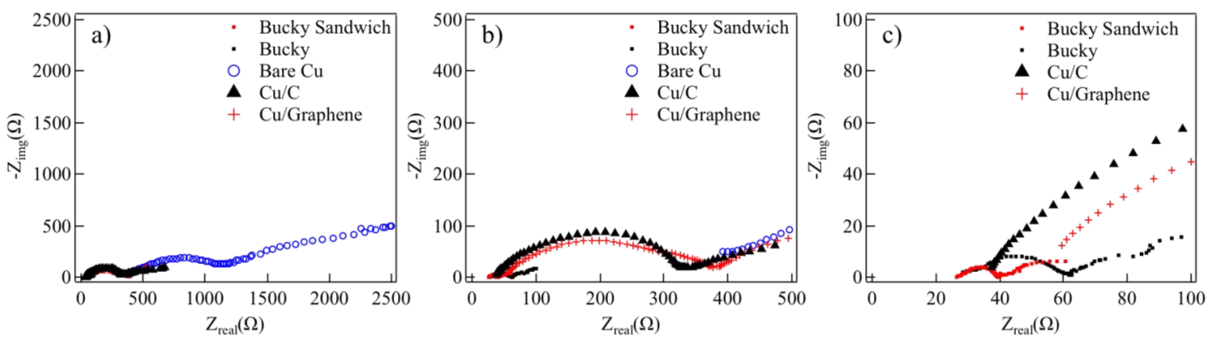

Figure S2: a) EIS spectra of all electrode at 0.1V for the first irreversible cycles. b) and c) Zoomed in for better viewing

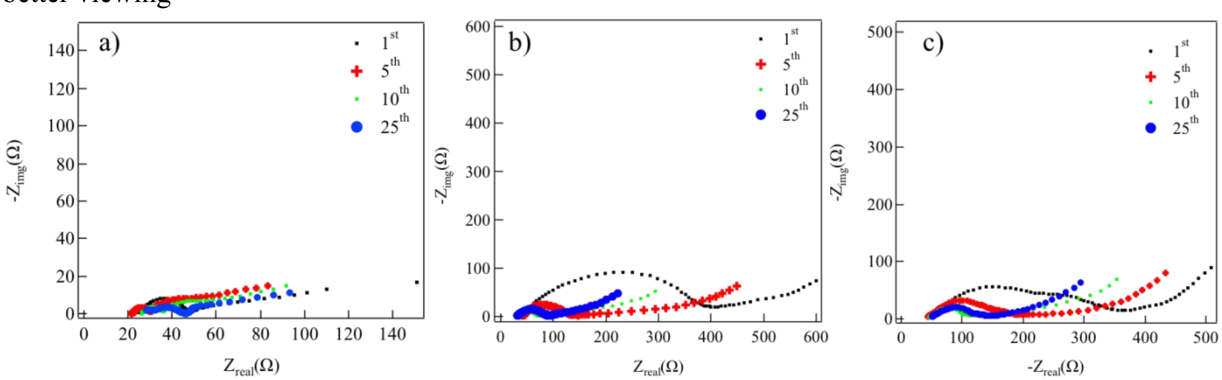

Figure S3: The EIS data for 1-25 cycles for a) Bucky b) Cu/C and c) Cu/graphene electrodes.

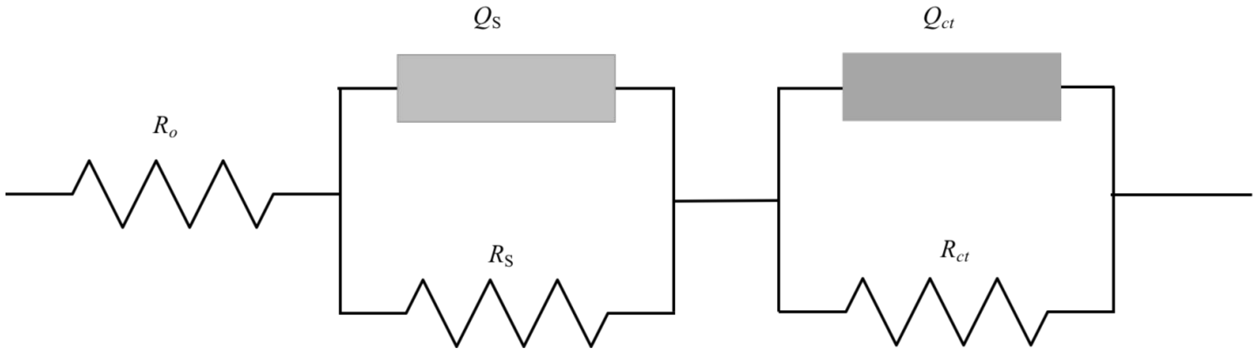

Figure S4: Equivalent circuit model used for fitting EIS data. Here R_o, R_s, and R_{ct} are the resistance due to bulk electrolyte, SEI layer and charge transfer. Q_s and Q_{ct} are respective constant phase elements.

Table S1: Fitting results of each component from equivalent circuit used in Figure S1.

Electrode	Cycle #	R_o (Ω)	R_{ct} (Ω)	R_s (Ω)	Q_{ct} (F.S^{-1})	a_{ct}	Q_s (F.S^{-1})	a_s
Bucky Sandwich	0	27.5	11.7	26.5	5.58E-05	0.75	0.125	0.57
	1	22.3	18.2	30.2	5.71E-05	0.86	0.072	0.49
	5	22.3	7.5	8.4	5.20E-04	0.67	0.640	0.72
	10	20.1	9.4	4.4	1.99E-04	0.76	0.049	0.81
	25	32.3	25.9	38.6	7.02E-04	0.52	0.072	0.80
Bucky	0	29.3	31.9	55.3	7.06E-05	0.63	0.0557	0.58
	1	25.5	22.9	46.7	9.66E-05	0.75	0.071	0.82
	5	22.1	7.4	57.3	1.22E-04	0.86	0.040	0.57
	10	26.5	8.7	57.9	1.39E-04	0.83	0.038	0.54
	25	26.8	21.4	27.6	1.34E-03	0.43	0.179	0.92
Bare Cu	0	366.0	798.5	1861.0	1.96E-05	0.51	7.96E-04	0.54
	1	379.0	652.9	1508.0	1.55E-05	0.56	1.19E-03	0.46
	5	361.0	618.4	1349.0	1.42E-05	0.57	1.16E-03	0.49
	10	367.0	656.5	1349.0	1.30E-05	0.58	1.10E-03	0.51
	25	390.0	643.6	1413.0	1.39E-05	0.57	8.18E-04	0.56
Cu/C	0	34	315.6	278.8	4.06E-05	0.625	1.30E-02	0.60
	1	40.15	359.0	239.6	5.40E-05	0.6195	1.02E-02	0.5-
	5	41.28	95.5	242.8	1.01E-04	0.6417	7.00E-03	0.42
	10	32.39	42.6	137.3	2.14E-04	0.6239	2.18E-02	0.35
	25	30.68	58.7	121.5	1.61E-04	0.592	2.44E-02	0.33
Cu/Graphene	0	44.55	313.0	636.5	3.55E-05	0.5373	1.28E-02	0.45
	1	38.59	204.7	590.9	5.28E-05	0.5849	4.56E-03	0.25
	5	43.09	124.4	594.2	7.32E-05	0.605	1.01E-02	0.39
	10	44.06	71.1	357.3	1.25E-04	0.6034	1.60E-02	0.53

	25	48.90	73.4	318.1	9.49E-05	0.5828	1.37E-02	0.41

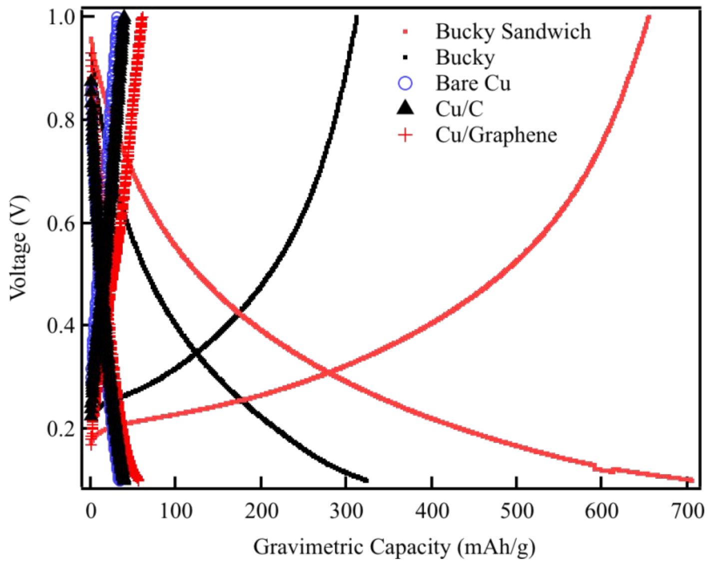

Figure S5: Charge and discharge profiles for all electrodes for 25th cycle at 0.1C rate

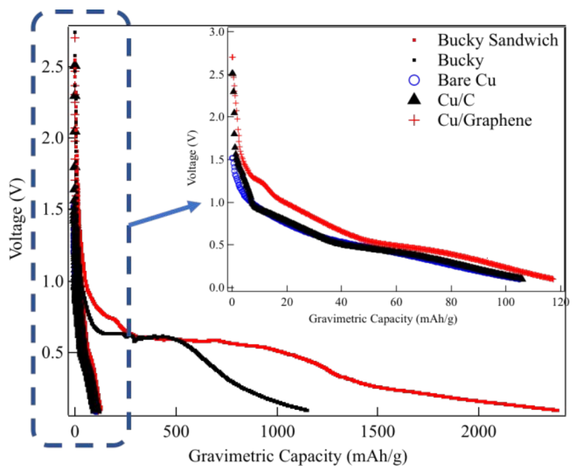

Figure S6: Discharge curves for all the electrodes in this study showing irreversible capacity loss. The inset shows a magnified view of the discharge curves <120 mAh/g

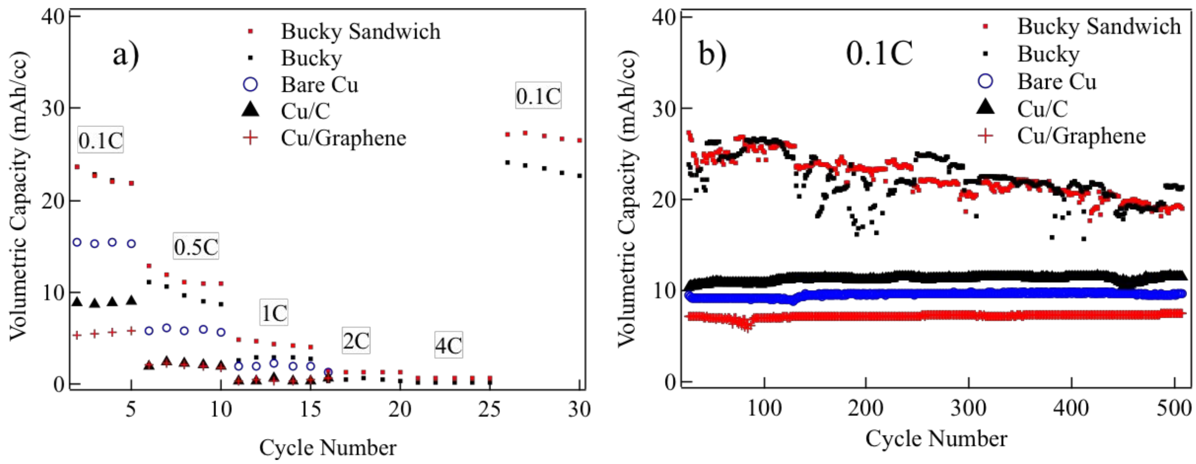

Figure S7: Volumetric rate capability tests of coin cells made of electrodes used in this study, (b) Cyclability of electrodes used in this study at 0.1C rate

Table S2: A table comparing the initial and final capacities of Bucky sandwich electrodes with other Si-based electrodes of similar mass density

Material	SiNPs diameter (nm)	Mass loading (mg/cm^2)	Operating Voltage (V)	Initial / Final capacity (mAh/g)	Cycle/ Current density (mA/g)	Ref.
Bucky paper/Si/Bucky paper sandwich	30	1.0	0.01-1.0	2900/1635	100/420	This work
Graphene/ Si nanocomposite	50	1.0	0.01-1.0	1050/815	100/500	[1]
Si/ N_2-doped C/ CNT sphere	50	0.8-1.0	0.01-1.5	1380/1031	100/500	[2]
3D Si/C fiber paper electrode	<100	0.95	0.02-1.5	1600/1178	100/500	[3]
3D Si/C fiber paper electrode	<100	1.22	0.02-1.5	1600/1267	100/500	[3]
Porous carbon matrix-Si	15	0.5-1.0	0.01-1.2	1215/1249	100/500	[4]
Mesoporous Si@SiO_2	NA	0.7-1.2	0.005-1.5	2789/1470	100/360	[5]
Adhesive polymer binder-Si	70	1.2	0.01-3.0	2811/2080	100/360	[6]
PAA binder-Si	70	1.2	0.01-3.0	2811/1068	100/360	[6]
Mesoporous carbon-Si/C	50-200	1.0-2.0	0.01-1.5	751/581	100/200	[7]
N_2 rich porous carbon framework-Si	30	1.0	0.01-1.5	1470/1103	100/100	[8]

References:

(1) Maroni, F.; Raccichini, R.; Birrozzi, A.; Carbonari, G.; Tossici, R.; Croce, F.; Marassi, R.; Nobili,

F. Graphene/Silicon Nanocomposite Anode with Enhanced Electrochemical Stability for Lithium-Ion Battery Applications. *J. Power Sources* 2014, *269*, 873–882.

(2) Zhang, Y. C.; You, Y.; Xin, S.; Yin, Y. X.; Zhang, J.; Wang, P.; Zheng, X. sheng; Cao, F. F.; Guo, Y. G. Rice Husk-Derived Hierarchical Silicon/Nitrogen-Doped Carbon/Carbon Nanotube Spheres as Low-Cost and High-Capacity Anodes for Lithium-Ion Batteries. *Nano Energy* 2016, *25*, 120–127.

(3) Xu, Y.; Zhu, Y.; Han, F.; Luo, C.; Wang, C. 3D Si/C Fiber Paper Electrodes Fabricated Using a Combined Electrospray/Electrospinning Technique for Li-Ion Batteries. *Adv. Energy Mater.* 2015, *5* (1), 1400753.

(4) Wu, L.; Yang, J.; Zhou, X.; Zhang, M.; Ren, Y.; Nie, Y. Silicon Nanoparticles Embedded in a Porous Carbon Matrix as a High-Performance Anode for Lithium-Ion Batteries. *J. Mater. Chem. A* 2016, *4* (29), 11381–11387.

(5) Liang, J.; Li, X.; Hou, Z.; Zhang, W.; Zhu, Y.; Qian, Y. A Deep Reduction and Partial Oxidation Strategy for Fabrication of Mesoporous Si Anode for Lithium Ion Batteries. *ACS Nano* 2016, *10* (2), 2295–2304.

(6) Pan, Y.; Ge, S.; Rashid, Z.; Gao, S.; Erwin, A.; Tsukruk, V.; Vogiatzis, K. D.; Sokolov, A. P.; Yang, H.; Cao, P.-F. Adhesive Polymers as Efficient Binders for High-Capacity Silicon Electrodes. *Cite This ACS Appl. Energy Mater* 2020, *2020*, 3387–3396.

(7) Shen, T.; Xia, X. H.; Xie, D.; Yao, Z. J.; Zhong, Y.; Zhan, J. Y.; Wang, D. H.; Wu, J. B.; Wang, X. L.; Tu, J. P. Encapsulating Silicon Nanoparticles into Mesoporous Carbon Forming Pomegranate-Structured Microspheres as a High-Performance Anode for Lithium Ion Batteries. *J. Mater. Chem. A* 2017, *5* (22), 11197–11203.

(8) Shi, L.; Wang, W.; Wang, A.; Yuan, K.; Jin, Z.; Yang, Y. Si Nanoparticles Adhering to a Nitrogen-Rich Porous Carbon Framework and Its Application as a Lithium-Ion Battery Anode Material. *J. Mater. Chem. A* 2015, *3* (35), 18190–18197.